polymers

MDPI

Article

Leads from Physical, Chemical, and Thermal Characterization on Cytotoxic Effects of Xylan-Based Microparticles

Henrique Rodrigues Marcelino [1,2], Acarília Eduardo da Silva [2], Monique Christine Salgado Gomes [1], Elquio Eleamen Oliveira [3], Toshiyuki Nagashima-Junior [4], Gardênia Sousa Pinheiro [5], Acarízia Eduardo da Silva [6], Ana Rafaela de Souza Timoteo [6], Lucymara Fassarela Agnez-Lima [6], Alejandro Pedro Ayala [7], Anselmo Gomes Oliveira [8] and Eryvaldo Sócrates Tabosa do Egito [1,2,*]

Received: 11 June 2015 ; Accepted: 3 August 2015 ; Published: 16 November 2015
Academic Editor: Francoise Winnik

1 Programa de Pós-graduação em Ciências Farmacêuticas (PPgCF), Universidade Federal do Rio Grande do Norte (UFRN), Natal/RN 59010-180, Brazil; henrique.rmarcelino@gmail.com (H.R.M.); moniquesalgado@gmail.com (M.C.S.G.)
2 Programa de Pós-graduação em Ciências da Saúde (PPgCSa), Universidade Federal Rio Grande do Norte (UFRN), Natal/RN 59010-180, Brazil; acariliasilva@gmail.com
3 Laboratório de Síntese e Vetorização de Moléculas, Centro de Ciências Biológicas e Sociais Aplicadas, Universidade Estadual da Paraíba (UEPB), João Pessoa/PB 58070-450, Brazil; elquioeleamen@yahoo.com.br
4 Centro de Educação e Saúde-Campus Avançado de Cuité, Universidade Federal de Campina Grande (UFCG), Cuité/PB 59175-000, Brazil; tonagashima@yahoo.com.br
5 Departamento de Física, Campus Ministro Petrônio Portella, Universidade Federal do Piauí, Teresina/PI 64049-550, Brazil; gardenia@fisica.ufc.br
6 Departamento de Biologia Celular e Genética, Universidade Federal do Rio Grande do Norte (UFRN), Natal/RN 59010-180, Brazil; acarizia@gmail.com (A.E.S.); arstimoteo@yahoo.com.br (A.R.S.T.); lfagnez@ufrnet.br (L.F.A.-L.)
7 Departamento de Física, Universidade Federal do Ceará (UFC), Fortaleza/CE 60020-181, Brazil; ayala@fisica.ufc.br
8 Departamento de Fármacos e Medicamentos, Faculdade de Ciências Farmacêuticas, Universidade do Estado de São Paulo (UNESP), Araraquara/SP 14801-902, Brazil; ans_gomes@yahoo.com.br
* Correspondence: socratesegito@gmail.com; Tel.: +55-84-3342-9817; Fax: +55-84-3342-9809

Abstract: Interfacial cross-linking (ICL) has been considered a feasible technique to produce polysaccharide-based microparticles (PbMs), even though only a few studies have been concerned with their biocompatibility. In this work, PbMs were prepared by the ICL method and characterized in regard to their *in vitro* biocompatibility, chemical linkages, and physical and thermal properties. First, the cell viability assay revealed that PbMs toxicity was concentration-dependent. Then, it was observed that the toxicity may be related to the way in which the binding occurred, and not exclusively to the stoichiometry between the polymer and the cross-linking agent. Moreover, the PbMs biosafety was predicted by the use of physicochemical procedures, which were able to identify unbound cross-linking agent residues and also to reveal the improvement of their thermal stability. Accordingly, this work suggests a step-by-step physicochemical procedure able to predict potential toxicity from micro-structured devices produced by polysaccharides. Likewise, the use of PbMs as a drug carrier should be cautiously considered.

Keywords: biocompatibility; interfacial cross-linking; polysaccharide; terephthaloyl chloride; microparticles

1. Introduction

The interfacial cross-linking method (ICL) has been considered a feasible technique to produce polysaccharide-based microparticles (PbMs) since the late 1970s [1]. This technique is based on the preparation of an emulsion as the first step, followed by a chemical reaction that occurs at the emulsion interface, which works as a microreactor to control the process and avoid the formation of chemically bounded aggregates [2].

Combined with the ICL technique, many cross-linkers have been extensively used to produce PbMs. Among them, epichlorohydrin, phosphoryl chloride, terephthaloyl chloride, and glutaraldehyde have been drawing more attention due to the good stability of the resulting particles. In spite of that, all those molecules have been reported as toxic when in their pure state [2–4].

Xylan is a polysaccharide extracted from hardwoods and annual plants, composed of a D-xylopyranose backbone chain with glucuronic acid, L-arabinose, and other sugars. Due to its complex structure, this polymer is insoluble in different media at both acid and neutral pH. Indeed, xylan's application in the pharmaceutical field has been studied mainly for colon-targeted drug delivery. When administered by the oral route, this polysaccharide is only degradable at the ascendant and transversal colon region due to the presence of bacteria that produce and excrete xylanases into the gastrointestinal tract [5,6]. However, its use as a raw material for the production of drug delivery systems has emerged in the recent literature [7,8]. Our group has also evaluated the production of colon-targeted drug carriers as a promising application for xylan [9,10].

The development of colon-targeted drug delivery systems has its focus in the treatment of local pathologies such as inflammatory bowel diseases and cancer. Such a strategy also has been used to enhance the bioavailability of peptides and proteins by the protection of such compounds in the gastrointestinal tract and by permeation through the wider tight junctions of this tissue [11].

The aim of this work was to evaluate the effect of ICL on xylan's biosafety and establish possible correlations among its physical, chemical, and thermal properties.

2. Experimental Section

2.1. Materials

Terephthaloyl chloride (TC), sorbitan triestearate (Span® 65), polysorbate 20 (Tween® 20), polysorbate 80 (Tween® 80), and a 3-(4,5-dimethylthiazol-2-yl)-2,5-diphenyltetrazolium bromide (MTT) kit were purchased from Sigma-Aldrich Chemical (St. Louis, MO, USA). Sodium hydroxide, chloroform, cyclohexane, and ethanol came from Vetec Chemical (Rio de Janeiro, Brazil). Dulbecco's modified eagle medium (DMEM) was obtained from Gibco® (Gaithersburg, MD, USA). Xylan was obtained after extraction from corn cobs as previously described by our group [12].

2.2. Microparticle Production

PbMs were produced by the ICL method as previously reported by Nagashima-Junior and colleagues [9]. Briefly, an alkali xylan solution was added into a chloroform:cyclohexane (1:4, v/v) mixture in order to obtain a W/O emulsion and then cross-linked using TC (Figure 1). According to the chemical composition of xylan from corn cobs described by Melo-Oliveira *et al.*, the ratio of hydroxyl radicals to TC molecules was 4.7×10^{-4} (molecules of xylan/molecules of TC) [13]. The PbMs were then washed three times with (1) an ethanolic solution containing 2% (v/v) polysorbate (Tween® 80 and Tween® 20, 1:1); (2) an ethanolic aqueous solution, 95 °GL; and (3) distilled water. After washing, the PbMs were dispersed into 50 mL of water. Afterwards, five samples containing 10 mL of PbMs were subjected to an ultra-rapid freezing process by immersion in liquid nitrogen (T = −196 °C) for 5 min. Freeze-drying was performed in an Alpha 1-2 freeze-dryer (Christ, Osterode, Germany) at −63 °C and 0.0018 mbar for 24 h to allow a complete freeze-drying cycle.

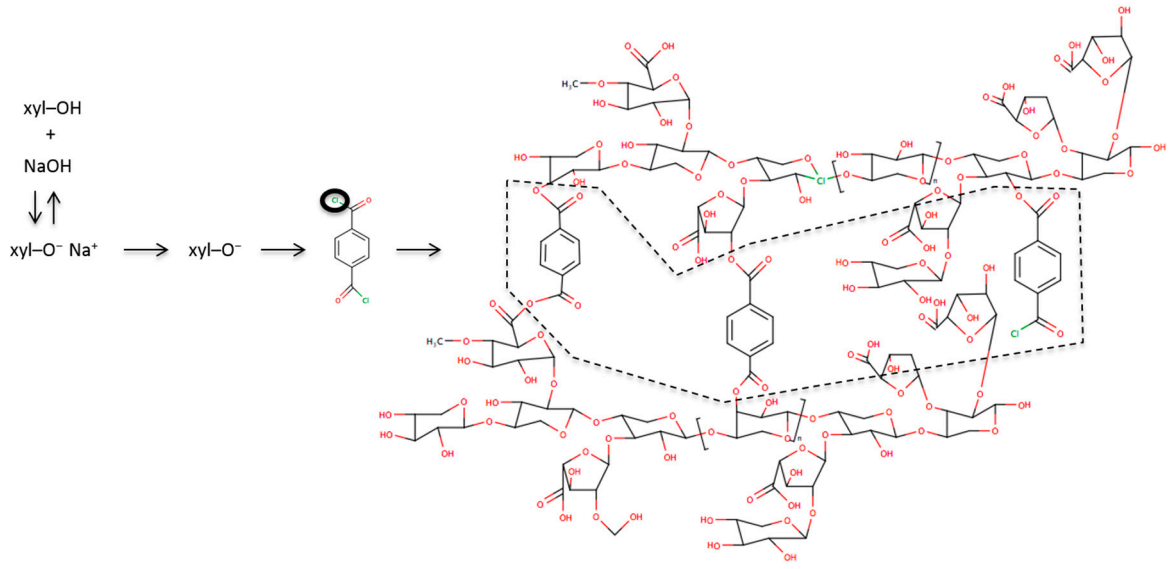

Figure 1. Scheme of cross-linking reaction between xylan and terephthaloyl chloride. The dashed polygon (—) highlight the linkage between terephthaloyl chloride molecules and xylan chains. The black circle represents the chlorine that is lost by the terephthaloyl chloride molecule during the cross-linking reaction.

2.3. Xylan Dispersions for Biocompatibility Assay

Xylan dispersion at 49.6 mg· mL^{-1} was prepared, under magnetic stirring, by the addition of xylan powder into a known amount of distilled water. Then, all dilutions utilized were produced according to the values described in Table 1.

Table 1. Chart of products used in the *in vitro* biocompatibility assay.

Tested product	Dilutions (Product:DMEM, *v*/*v*)
Xylan dispersion in water (49.8 mg· mL^{-1} of xylan)	1:1 (corresponding to 24.8 mg· mL^{-1}) 1:3 (corresponding to 12.4 mg· mL^{-1}) 1:7 (corresponding to 6.2 mg· mL^{-1}) 1:15 (corresponding to 3.1 mg· mL^{-1})
PbMs suspension in water (1.488 mg· mL^{-1} of xylan)	1:1 (corresponding to 0.744 mg· mL^{-1}) 1:3 (corresponding to 0.372 mg· mL^{-1}) 1:7 (corresponding to 0.186 mg· mL^{-1}) 1:15 (corresponding to 0.093 mg· mL^{-1}) 1:31 (corresponding to 0.0465 mg· mL^{-1})

2.4. Morphology and Particle Size Distribution Analysis

The PbMs morphology was evaluated by scanning electronic microscope (XL 30 ESEM, Phillips, Amsterdam, Netherlands). The particle analysis was carried out by dynamic laser scattering (920L Cilas, Beckman Colter, Villepinte, France). The span index was also evaluated by the following equation:

$$\text{Span Index} = (\text{D90} - \text{D10})/\text{D50} \quad (1)$$

where D90, D10, and D50 are the particle sizes determined to the 90th, 50th, and 10th percentile of undersized particles, respectively.

2.5. Powder X-ray Diffraction (XRD)

XRD analyses were performed for the xylan powder, TC, and PbMs using an XRD-6000 diffractometer (Shimadzu, Kyoto, Japan) with a 2θ range between 20° and 80° using Cu Kα radiation (λ = 1.54056 Å). The XRD patterns were recorded at room temperature.

2.6. Fourier Transform Infrared (FT-IR) Spectroscopy

The FT-IR analyses were performed in solid state with a Nicolet Nexus 470 FT-IR spectrometer (Thermo Scientific, Waltham, MA, USA). The xylan powder and the PbMs dried samples were crushed with KBr and compressed into pellets. Spectral scanning was run in the range of 4000 to 400 cm^{-1}. Prior to recording, the spectra were transformed against a KBr background.

2.7. Thermal Analysis

Thermogravimetry analysis (TGA) and derivative thermogravimetric curve (DTG) were obtained with an STA 409 PC Luxx device (Netzsch, Selb, Germany), using an aluminum pan with about 5 mg of sample under dynamic nitrogen atmosphere (10 $mL \cdot min^{-1}$) at the heating rate of 10 $°C \cdot min^{-1}$, from 25 to 600 °C. Differential scanning calorimetry (DSC) curves were obtained with a Phoenix 204 calorimeter (Netzsch, Selb, Germany) using an aluminum pan with about 5 mg of sample under dynamic nitrogen atmosphere (10 $mL \cdot min^{-1}$) at a heating rate of 10 $°C \cdot min^{-1}$, from 25 to 600 °C.

2.8. In Vitro Biocompatibility Assay

To evaluate the biocompatibility of the formulation (PbMs) and its raw material (xylan), the metabolic activity was measured by 3-(4,5-dimethylthiazol-2-yl)-2,5-diphenyltetrazolium bromide (MTT) assay. Firstly, human cervical adenocarcinoma cells (5×10^4 HeLa cells/well) were plated on 96-well microplates and were treated with 200 µL of the tested dispersions (Table 1) for 24 h at 5% CO_2 and 37 °C.

The control cells were incubated with only DMEM medium under the same conditions. The MTT was dissolved in sterile PBS at 0.5 mg/mL. Then, 100 µL of the MTT solution was added into each well after removing old culture medium and washed twice with PBS at 37 °C, followed by incubation at 5% CO_2 atmosphere and 37 °C for 2 h. After removing the MTT reagent, 100 µL of dimethyl sulfoxide (DMSO) was added to dissolve the purple formazan crystal inside the cells. Finally, the absorbance of the purple formazan crystal in DMSO was measured at 540 nm wavelength using a microplate reader (µQuant™, Bio-Tek instruments, Winooski, VT, USA), and cell viability was expressed as ratios *versus* untreated cells ($OD_{Control}/OD_{Sample} = 100\%/x$), where "$x$" is the percentage value for the cell viability tested with samples. All samples were tested in 15 and 18 replicates for each concentration of PbMs and xylan, respectively.

2.9. Statistical Analysis

To evaluate the data obtained from the *in vitro* biocompatibility assay, a one-way ANOVA was performed, followed by the Tukey *post hoc* test. A p-value less than 0.05 was assumed for the statistically significant differences. Moreover, linear regressions were performed to better describe data behavior. For all analyses, RStudio version 0.98.501 was used with the following packages loaded: lattice, ggplot2, and pwr.

3. Results and Discussion

The development of PbMs as potential drug carriers by ICL with TC has been reported over the last two decades [14,15]. However, a small number of papers investigated the biocompatibility of these systems, and only a few of them showed success in its biological application [16–18]. In

the following sections, PbMs biocompatibility will be described and possible correlations among physical, chemical, and thermal properties with their biosafety will be discussed.

3.1. Physical and Chemical Characterization

3.1.1. Morphology and Size Distributions

The scanning electron microscopy (SEM) images revealed PbMs defined by a tiny polymeric membrane, a smooth surface, and an oblong shape (Figure 2a,b). No aggregates were observed, although many broken PbMs were found. This probably occurred because the freeze-drying process is a stressing process and involves ice crystal formation and ice sublimation that can disrupt the complex structure of the PbMs as observed in other freeze-dried microparticles [19]. Also, Nagashima *et al.* observed no broken structures in the PbMs morphology evaluation by optical microscopy.

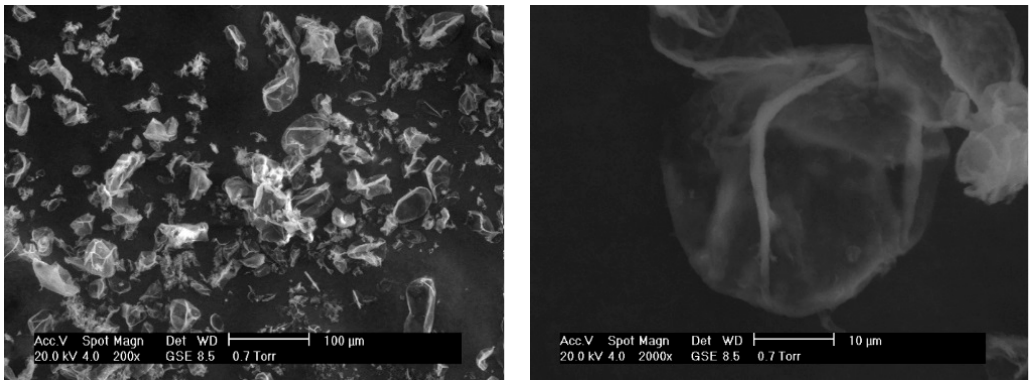

(**a**) (**b**)

Figure 2. SEM images of polysaccharide-based microparticles after freeze-drying at (**a**) 200×; and (**b**) 2000×.

The PbMs presented symmetric distribution as might be observed by the particle size distribution analysis (Figure 3a,b). In fact, 10%, 50% and 90% of the microparticle samples were smaller than 13, 34 and 63 µm, respectively. Also, the mean particle diameter was found to be 37 µm (Figure 3a). The mean particle sizes of 10%, 50%, and 90% of PbMs before freeze-drying were smaller than 14, 41 and 74 µm, respectively, and their mean diameter was 43 µm (Figure 3b). The span index for both formulations was found to be 1.47, indicating good control over the particle size distribution using the ICL method [20].

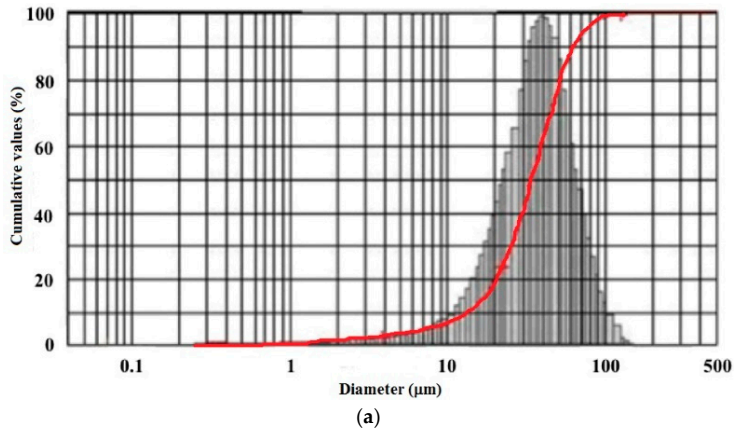

(**a**)

Figure 3. *Cont.*

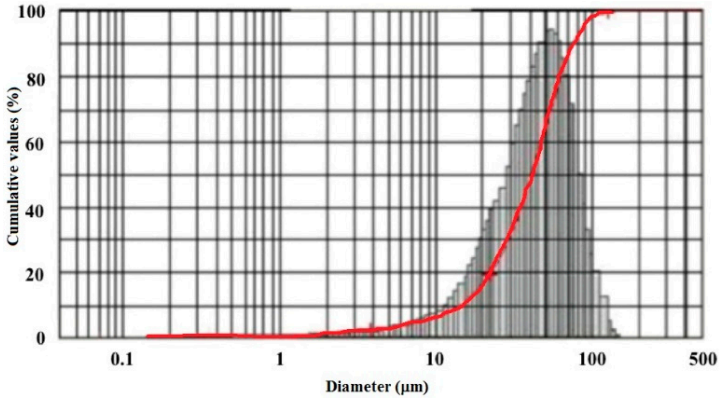

(**b**)

Figure 3. (**a**) Size distribution of polysaccharide-based microparticles before; and (**b**) after the freeze-drying process. The red line present the cumulative index line.

3.1.2. FT-IR Spectroscopy

The infrared analyses were performed in order to observe the formation of terephthalic esters bound to the PbMs due to the reaction between the cross-linking agent and the xylan. Initially, the xylan infrared spectrum (Figure 4) was found to be similar to those reported by our group and elsewhere [12,21]. Concerning the FT-IR spectrum of PbMs, peaks ascribed for polysaccharides were also detected. Moreover, an absorption band at 1280 cm^{-1}, which can be attributed to the halogen bond in the carbonyl group of the TC structure, was detected (Figure 4). Also detected was a peak at 1724 cm^{-1}, which is attributed to C=O stretching vibrations related to the aromatic acid esters, such as terephthalic esters [16,22]. The presence of terephthalic esters on the PbMs spectrum is evidence of the cross-linking reaction between xylan and TC, which is the reason for the polymeric membrane stabilization since no other known approach for cross-linking, such as heating, pressure, or UV light exposure, was used to reinforce the polymer chains [23].

Additionally, the halogen bond identified at the PbM spectrum corroborates with the hypothesized mechanism of toxicity, as described in the Cell Viability through MTT assay section. The toxicity appears to be related to the cross-linking agent molecules that are bound to xylan, but would remain with some unreacted radicals free to react with the media.

3.1.3. XRD Analysis

XRD has been reported as a helpful tool to strengthen the results from the FT-IR spectroscopy because cross-linking agents usually show crystallinity while polymers are described as amorphous compounds [24,25]. As previously suggested by Oliveira and colleagues, the XRD analysis of xylan presented a profile of amorphous polymers displaying no crystallinity peaks. On the other hand, the cross-linking agent showed several peaks due to its crystallinity [12] (Figure 5a,b). In fact, the analysis of PbMs detected two peaks with different intensities near the angle for TC peaks [25]. The absence of other peaks from TC suggests that the molecules self-arranged while maintaining a minimal crystallinity. However, the crystallinity observed in the PbMs may be due to the organization of the xylan chains after the cross-linking reaction with TC, which might be an additional factor together with the unreacted TC radicals observed by FT-IR, as the reason for PbMs toxicity.

Indeed, the results from the cell viability, FT-IR, and XRD showed that the toxicity of PbMs is related with the cross-linking of xylan, which may not be merely related to the stoichiometry between the cross-linking agent and the polymer, but to the way in which the TC acts on the binding. Moreover, the toxicity could also be predicted by using a step-by-step physicochemical procedure to identify the crystalinity changes that might induce toxicity.

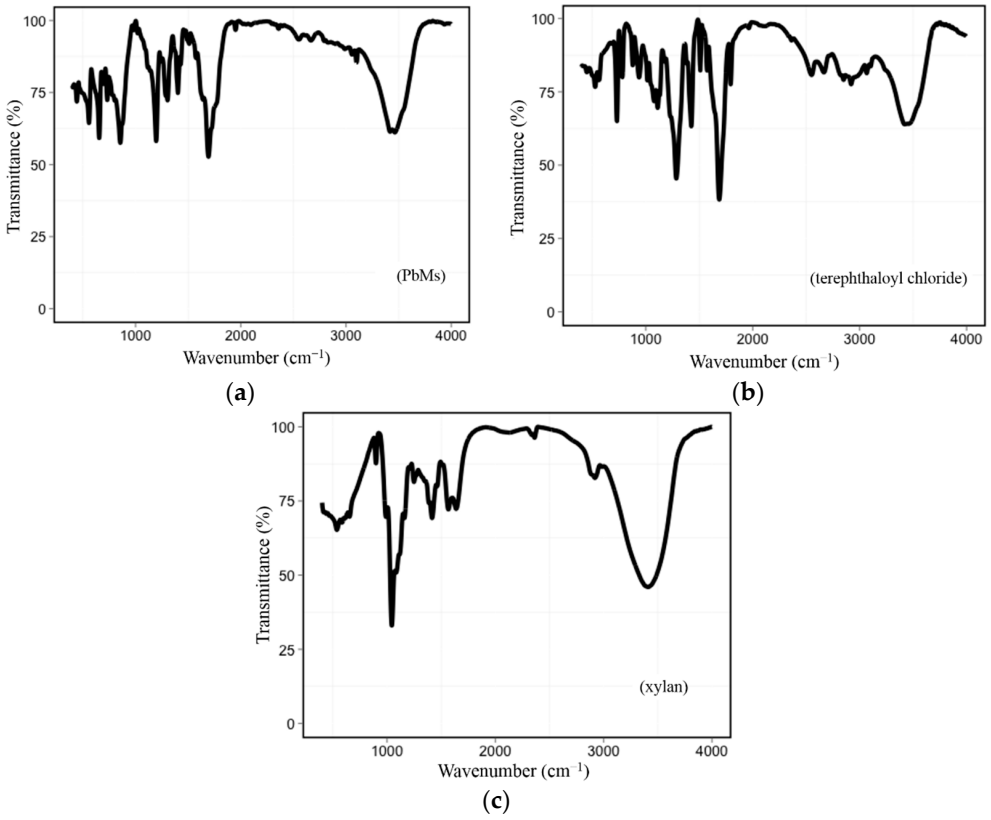

Figure 4. (**a**) FT-IR spectra of polysaccharide-based microparticles; (**b**) terephthaloyl chloride; and (**c**) and xylan.

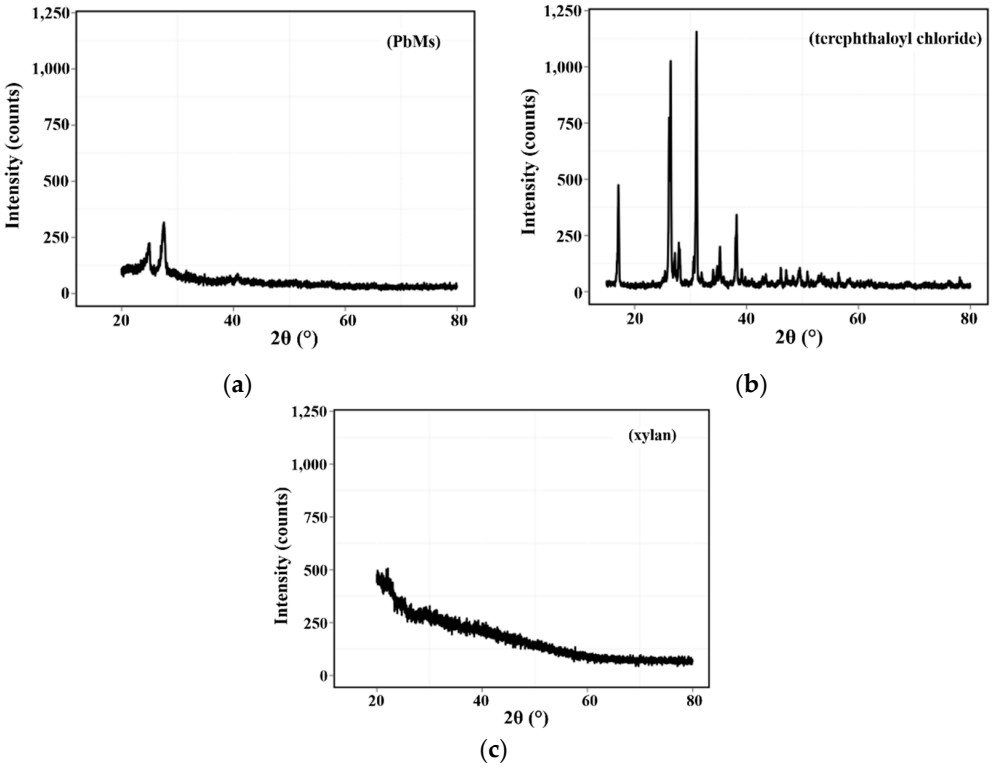

Figure 5. (**a**) XRD curves of polysaccharide-based microparticles; (**b**) terephthaloyl chloride; and (**c**) xylan powder.

3.1.4. Thermal Analysis

Even though PbMs revealed to be more toxic than xylan itself, and similar citotoxicity has been described in starch microcapsules [14], its use at low concentrations might be considered for drugs with high potency, where the administration of PbMs would be reduced due to the low payload of the drug. For this reason, the analyses of the PbMs thermal characteristics were carried out.

The TGA of xylan powder (Figure 6a) showed two steps of mass loss, −8.9% and −49.8% at 55–150 °C and 180–380 °C, respectively. These events were clearly fingerprinted on the DTG curve, where a small shoulder in the second mass loss event suggests that it is a two-stage process (Figure 6a). The first event, occurring between 100 and 150 °C, may be related to hydration water loss from the xylan powder. The main event, occurring subsequently at higher temperatures up to about 380 °C, is related to the onset of polymer degradation processes.

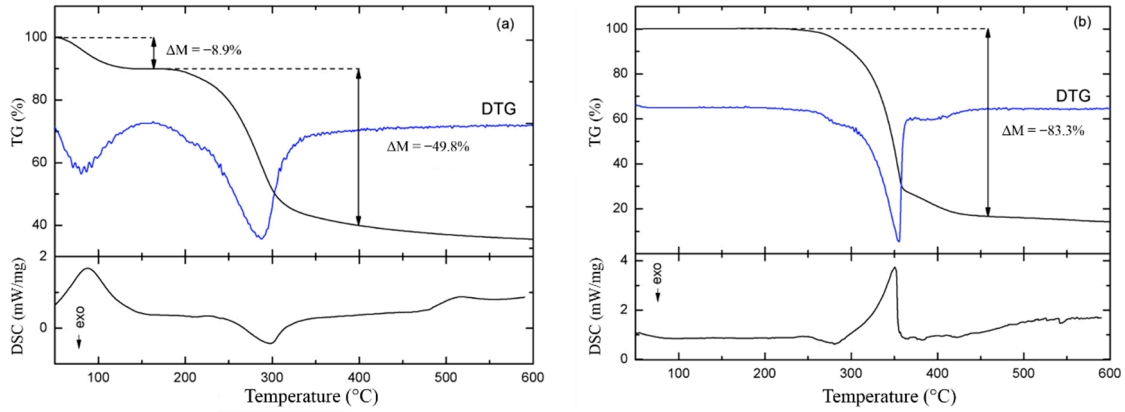

Figure 6. (**a**) TGA and DSC curves of xylan powder; and (**b**) polysaccharide-based microparticles.

These results are in agreement with the complex structure of carbohydrates, which have a degradation process determined by dehydration reactions such as desorption of physically adsorbed water and removal of structural water, respectively. Additionally, depolymerization followed by rupture of C–O and C–C bonds in the ring units, such as of 4-*O*-methylglucuronic acid and acetyl groups, results in the increase of CO, CO_2, and H_2O, and the formation of polynuclear aromatic and graphitic structures [26–29]. Thus, the observed events can be related to the release of water and the pyrolysis of xylan. The xylan pyrolysis was driven by the evolution of several volatile gasses as shown by Shen *et al.* [27]. Both mass loss processes were also evidenced in the DSC curves by an endothermic and an exothermic peak, respectively (Figure 6a). A third endothermic event had an onset temperature of 485.5 °C. Even though it has no counterpart in the TGA curve, this event could be related to the CH_4 evolving, as observed by Shen *et al.* [27], at the same temperature.

On the other hand, the TGA of PbMs showed only a one-step mass loss of 83.3% between 230 °C and 450 °C (Figure 6b). Similar to the previous case, the DTG curve showed that three subsequent events were involved in the PbMs decomposition. These events were clearly observed in the DSC curves as an exothermic peak was followed by an endothermic one. The third event, a weak shoulder after the main mass loss process, was not observed in the DSC curve, probably because of the little residual mass resulting from the decomposition. The different thermal behaviors of xylan and PbMs at 100 °C may be a consequence of the freeze-drying process that removes almost all water content from the PbMs dispersion. Additionally, the increase in the temperature of degradation for PbMs may be related to the complexation between the cross-linking agent and the xylan. In fact, it has been demonstrated that TC is able to increase the thermal and mechanical properties of some materials in aerospace and military areas [30]. Thus, the only identified mass loss event is related to the breaking of the bonds between glycoside compounds and depolymerization [27].

These features are supported by the results of the FT-IR and the XRD analyses, which revealed the correlation between the polymer and the cross-link agent, and the crystallinity of PbMs.

3.2. Cell Viability through MTT Assay

The MTT assay, based on NAD(P)H-dependent cellular oxidoreductase activity, has been widely used for assessing cytotoxicity induced by several compounds in *in vitro* cell culture models [31]. The data obtained from the MTT assay showed that PbMs are more cytotoxic than xylan, since PbMs caused reduction in cell viability at lower concentrations than the ones used for xylan. To standardize the used xylan concentrations for PbMs samples (Table 1), 1.488 mg· mL^{-1} was considered as the initial studied concentration in this assay. This value corresponds to the initial amount of xylan in the final volume of the PbMs suspension.

Xylan was shown to be satisfactorily biocompatible in the range of 4.1–12.4 mg· mL^{-1}, as a cell viability degree of about 70% was found (Figure 7a,c). Indeed, these results were expected because this material is considered highly stable, nontoxic, and hydrophilic [10,32], even though anti-proliferative activity of xylan against HeLa cells has been reported as its AC50 = 1 mg/mL, as well as the activity of other polysaccharides [13]. Despite its low toxicity, at 24.8 mg· mL^{-1} the cell viability decreased (Figure 7a,c), probably as a result of the saturation of the medium with xylan and, consequently, the precipitation of xylan as result of its low solubility in aqueous medium at physiological pH [33]. Moreover, concerning the biosafety use of xylan in normal cells, this result might lead to the conclusion that concentrations smaller than 24.8 mg· mL^{-1} should be used. In fact, this prediction might be supported, as HeLa cells (used here as a model of study) are much less sensitive than the non-carcinogenic cells.

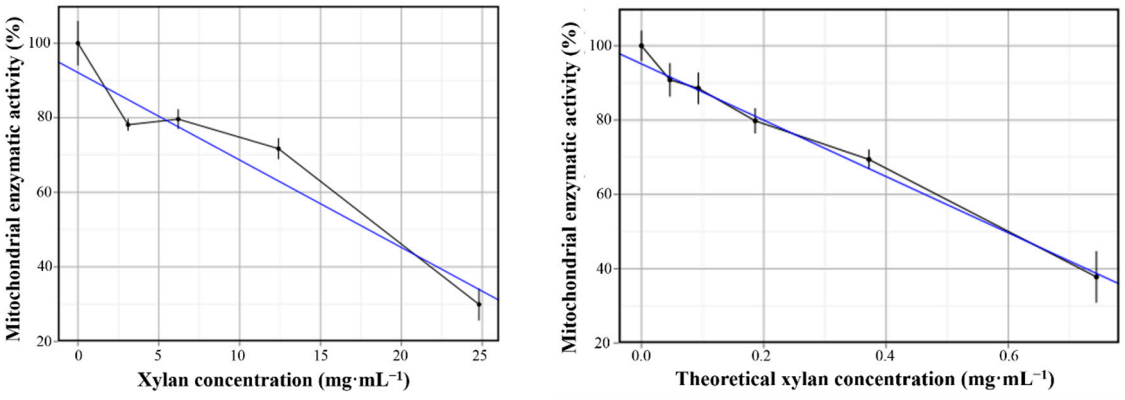

Figure 7. Cell viability of HeLa cells after 24 h incubation with xylan dispersions at different concentrations and polysaccharide-based microparticle (PbMs) dilutions. (**a**) Scatterplots for xylan dispersions; and (**b**) PbMs suspensions with trend lines. The lines in the graphics are the trending line (blue) and the direct line that connect all the points (black).

The cell viability in the presence of PbMs was close to 70% at the theoretical xylan concentration of 0.372 mg· mL^{-1} at the formulation (Figure 7b). The cytotoxicity exhibited by PbMs might be explained by the presence of the free unreacted radicals from TC, displayed in the FT-IR (Figure 4a). The chloride toxicity is induced due to its ability to oxidize the main cell components such as amino groups of amino acids [34].

Afterwards, the performance of the statistics analysis for different groups of xylan dispersion and PbMs suspensions showed *p*-values higher than 0.05 (Table S1). However, when concentration dependency was analyzed for xylan and PbMs separately, *p*-values smaller than 0.05 were observed. Therefore, a ratio between xylan concentration (for xylan dispersions) and the theoretical xylan

concentration (for PbMs suspensions) was performed. As a result, it was found that in order to present the same toxicity as PbMs, the xylan dispersion would have to be presented at 33.3-fold in the media. This ratio value supports the hypothesis that polysaccharides are safe as broadly reported [35]. Therefore, further physicochemical analyses were mandatory to identify eventual residues of the cross-linking agent, as previously mentioned.

Furthermore, the evaluation of the concentration of xylan dispersions and PbMs suspensions able to reduce the cell viability in 50% was calculated by the equation from the linear regression study (Figure 7, Table 2). The values of 17.93 and 0.59 mg· mL^{-1} were found for xylan dispersions and PbMs, respectively. The ratio between these concentrations was 30.27 mg· mL^{-1}, which is close to the value obtained in the analysis among the non-statistically different groups.

Overall, the statistical results pointed out the biosafety of the xylan polymer and the toxicity related to the cross-linking agent, TC, in the production of PbMs.

Table 2. Linear regression from cell viability *vs.* xylan concentrations in the xylan dispersions and in PbMs suspensions.

Sample	Slope (Angular Coefficient)	Intercept (Linear Coefficient)	R^2 (Determination Coefficient)
xylan	−2.35	92.12	0.895
PbMs	−75.79	95.13	0.944

4. Conclusions

This work suggests a step-by-step procedure to evaluate the biosafety of polysaccharides and the micro-structured devices produced with them. Moreover, xylan showed to be a biocompatible raw material for the production of microparticles. However, the use of TC as a cross-linking agent for the PbMs production prompts a meaningful reduction, approximately 30-fold, in its biocompatibility due to the residual chloride radicals. The FT-IR showed remains of a halogen bond, while XRD revealed that no crystals from TC remain in the particle. The evaluation of these results together suggests that the halogen-aromatic bond from TC would be the probable source of toxicity of PbMs. Additionally, the xylan cross-linking with TC would be the reason for PbMs crystallinity. Thermal analysis confirmed the formation of a more stable compound, as the temperatures to observe weight loss and the variation on enthalpy were higher for PbMs than for xylan itself, indicating that if biological safety is not a concern, the utilization of PbMs is chemically feasible. Furthermore, the ICL technique showed to be a very controlled process able to produce a short range of particle size distributions, as observed by the microscopy and particle size distribution. Finally, the ICL with TC seemed to be a viable technique for the production of drug carriers, although PbMs showed some toxicity. However, its good chemical, morphological, and thermal characteristics also provide a potential applicability in textile and tissue engineering.

Supplementary Materials: Supplementary materials can be accessed at: www.mdpi.com/2073-4360/7/11/1515/s1.

Acknowledgments: The authors are grateful to CAPES and CNPq for the financial support, to the Nucleo de Ensino e Pequisa em Gás natural (NEPGN, CT-INFRA/LIEM) for the DRX and SEM analysis, to Mária de Fátima Vitória de Moura for the FT-IR analysis, to Rosangela Balaban (Laboratóio de Petróleo, LAPET/UFRN) for the particle size analysis, and Glenn Hawes, M Ed. (Master of Education, University of Georgia) for editing this manuscript. Additionally, the authors are grateful to Gabrielle Daumen for figures quality improvement.

Author Contributions: Henrique Rodrigues Marcelino: Design of experiments, performance of experiments, data analysis, and writing of the manuscript; Acarília Eduardo da Silva: Data analysis and writing of the manuscript; Monique Christine Salgado Gomes: Performance of experiments; Elquio Eleamen Oliveira: Design of experiments, data analysis, and writing of the manuscript; Toshiyuki Nagashima-Junior: Data analysis and of writing the manuscript; Gardênia Sousa Pinheiro: Performance of experiments and data analysis; Acarízia Eduardo da Silva: Performance of experiments and data analysis; Ana Rafaela de Souza Timoteo: Performance of experiments and data analysis; Lucymara Fassarela Agnez-Lima: Data analysis and editing

manuscript; Alejandro Pedro Ayala: Data analysis and editing manuscript; Anselmo Gomes Oliveira: Editing manuscript; Eryvaldo Sócrates Tabosa do Egito: Concept of the Project, funding, and editing manuscript.

Conflicts of Interest: The authors declare no conflict of interest.

References

1. Rothman, U.; Arfors, K.E.; Aronsen, K.F.; Lindell, B.; Nylander, G. Enzymatically degradable microspheres for experimental and clinical use. In *Sixth Meeting of the Nordic Microcirculation Group*; Microvascular Research: Geilo, Norway, 1976; Volume 11, pp. 421–430.
2. Lévy, M.C.; Andry, M.C. Microcapsules prepared through interfacial cross-linking of starch derivatives. *Int. J. Pharm.* **1990**, *62*, 27–35. [CrossRef]
3. Jain, A.K.; Khar, R.K.; Ahmed, F.J.; Diwan, P.V. Effective insulin delivery using starch nanoparticles as a potential trans-nasal mucoadhesive carrier. *Euro. J. Pharm. Biopharm.* **2008**, *69*, 426–435. [CrossRef] [PubMed]
4. Patel, Z.S.; Yamamoto, M.; Ueda, H.; Tabata, Y.; Mikos, A.G. Biodegradable gelatin microparticles as delivery systems for the controlled release of bone morphogenetic protein-2. *Acta Biomater.* **2008**, *4*, 1126–1138. [CrossRef] [PubMed]
5. Dodd, D.; Mackie, R.I.; Cann, I.K. Xylan degradation, a metabolic property shared by rumen and human colonic bacteroidetes. *Mol. Microbiol.* **2011**, *79*, 292–304. [CrossRef] [PubMed]
6. Hansen, N.M.L.; Plackett, D. Sustainable films and coatings from hemicelluloses: A review. *Biomacromolecules* **2008**, *9*, 1493–1505. [CrossRef] [PubMed]
7. Daus, S.; Heinze, T. Xylan-based nanoparticles: Prodrugs for ibuprofen release. *Macromol. Biosci.* **2010**, *10*, 211–220. [CrossRef] [PubMed]
8. Petzold-Welcke, K.; Schwikal, K.; Daus, S.; Heinze, T. Xylan derivatives and their application potential—Mini-review of own results. *Carbohydr. Polym.* **2014**, *100*, 80–88. [CrossRef] [PubMed]
9. Nagashima-Junior, T.; Oliveira, E.E.; da Silva, A.E.; Marcelino, H.R.; Gomes, M.C.S.; Aguiar, L.M.; de Araujo, I.B.; Soares, L.A.; Oliveira, A.G.; Egito, E.S.T. Influence of the lipophilic external phase composition on the preparation and characterization of xylan microcapsules—A technical note. *Aaps PharmSciTech* **2008**, *9*, 814–817. [CrossRef] [PubMed]
10. Silva, A.E.; Oliveira, E.E.; Gomes, M.C.S.; Marcelino, H.R.; Silva, K.C.; Souza, B.S.; Nagashima-Junior, T.; Ayala, A.P.; Oliveira, A.G.; Egito, E.S.T. Producing xylan/Eudragit® s100-based microparticles by chemical and physico-mechanical approaches as carriers for 5-aminosalicylic acid. *J. Microencapsul.* **2013**, *30*, 787–795. [CrossRef] [PubMed]
11. Coco, R.; Plapied, L.; Pourcelle, V.; Jerome, C.; Brayden, D.J.; Schneider, Y.J.; Preat, V. Drug delivery to inflamed colon by nanoparticles: Comparison of different strategies. *Int. J. Pharm.* **2013**, *440*, 3–12. [CrossRef] [PubMed]
12. Oliveira, E.E.; Silva, A.E.; Nagashima-Junior, T.; Gomes, M.C.S.; Aguiar, L.M.; Marcelino, H.R.; Araujo, I.B.; Bayer, M.P.; Ricardo, N.M.; Oliveira, A.G.; *et al*. Xylan from corn cobs, a promising polymer for drug delivery: Production and characterization. *Bioresour. Technol.* **2010**, *101*, 5402–5406. [CrossRef] [PubMed]
13. Melo-Silveira, R.F.; Fidelis, G.P.; Costa, M.S.; Telles, C.B.; Dantas-Santos, N.; Oliveira Elias, S.; Ribeiro, V.B.; Barth, A.L.; Macedo, A.J.; Leite, E.L.; *et al*. *In vitro* antioxidant, anticoagulant and antimicrobial activity and in inhibition of cancer cell proliferation by xylan extracted from corn cobs. *Int. J. Mol. Sci.* **2012**, *13*, 409–426. [CrossRef] [PubMed]
14. Devy, J.; Balasse, E.; Kaplan, H.; Madoulet, C.; Andry, M.C. Hydroxyethylstarch microcapsules: A preliminary study for tumor immunotherapy application. *Int. J. Pharm.* **2006**, *307*, 194–200. [CrossRef] [PubMed]
15. Pariot, N.; Edwards-Levy, F.; Andry, M.C.; Levy, M.C. Cross-linked β-cyclodextrin microcapsules: Preparation and properties. *Int. J. Pharm.* **2000**, *211*, 19–27. [CrossRef]
16. Larionova, N.V.; Kazanskaya, N.F.; Larionova, N.I.; Ponchel, G.; Duchene, D. Preparation and characterization of microencapsulated proteinase inhibitor aprotinin. *Biochemistry* **1999**, *64*, 857–862. [PubMed]

17. Larionova, N.V.; Ponchel, G.; Duchene, D.; Larionova, N.I. Biodegradable cross-linked starch/protein microcapsules containing proteinase inhibitor for oral protein administration. *Int. J. Pharm.* **1999**, *189*, 171–178. [CrossRef]
18. Krasota, A.; Belousova, R.; Duchene, D.; Larionova, N. *In vitro* inhibition of bovine herpes virus 1 reproduction with native and microencapsulated proteinase inhibitor aprotinin. *J. Control. Release* **2002**, *85*, 117–124. [CrossRef]
19. Klose, D.; Siepmann, F.; Elkharraz, K.; Krenzlin, S.; Siepmann, J. How porosity and size affect the drug release mechanisms from pliga-based microparticles. *Int. J. Pharm.* **2006**, *314*, 198–206. [CrossRef] [PubMed]
20. Reynaud, F.; Tsapis, N.; Deyme, M.; Vasconcelos, T.G.; Gueutin, C.; Guterres, S.S.; Pohlmann, A.R.; Fattal, E. Spray-dried chitosan-metal microparticles for ciprofloxacin adsorption: Kinetic and equilibrium studies. *Soft Matter* **2011**, *7*, 7304. [CrossRef]
21. Kacurakova, M.; Capek, P.; Sasinkova, V.; Wellner, N.; Ebringerova, A. FT-IR study of plant cell wall model compounds: Pectic polysaccharides and hemicelluloses. *Carbohydr. Polym.* **2000**, *43*, 195–203. [CrossRef]
22. Silverstein, R.M.; Webster, F.X.; Kiemle, D.J. *Spectrometric Identification of Organic Compounds*, 7th ed.; John Wiley & Sons Inc.: Hoboken, NJ, USA, 2005.
23. Guan, J.; Ferrell, N.; James Lee, L.; Hansford, D.J. Fabrication of polymeric microparticles for drug delivery by soft lithography. *Biomaterials* **2006**, *27*, 4034–4041. [CrossRef] [PubMed]
24. Li, B.-Z.; Wang, L.-J.; Li, D.; Bhandari, B.; Li, S.-J.; Lan, Y.; Chen, X.D.; Mao, Z.-H. Fabrication of starch-based microparticles by an emulsification-crosslinking method. *J. Food Eng.* **2009**, *92*, 250–254. [CrossRef]
25. Li, B.-Z.; Wang, L.-J.; Li, D.; Chiu, Y.L.; Zhang, Z.-J.; Shi, J.; Chen, X.D.; Mao, Z.-H. Physical properties and loading capacity of starch-based microparticles crosslinked with trisodium trimetaphosphate. *J. Food Eng.* **2009**, *92*, 255–260. [CrossRef]
26. Parikh, A.; Madamwar, D. Partial characterization of extracellular polysaccharides from cyanobacteria. *Bioresour. Technol.* **2006**, *97*, 1822–1827. [CrossRef] [PubMed]
27. Shen, D.K.; Gu, S.; Bridgwater, A.V. Study on the pyrolytic behaviour of xylan-based hemicellulose using TG-FTIR and Py-GC-FTIR. *J. Anal. Appl. Pyrolysis* **2010**, *87*, 199–206. [CrossRef]
28. Shen, D.K.; Gu, S.; Bridgwater, A.V. The thermal performance of the polysaccharides extracted from hardwood: Cellulose and hemicellulose. *Carbohydr. Polym.* **2010**, *82*, 39–45. [CrossRef]
29. Wang, S.; Liu, Q.; Luo, Z.; Wen, L.; Cen, K. Mechanism study on cellulose pyrolysis using thermogravimetric analysis coupled with infrared spectroscopy. *Front. Energy Power Eng. China* **2007**, *1*, 413–419. [CrossRef]
30. Mitra, T.; Sailakshmi, G.; Gnanamani, A.; Mandal, A.B. Cross-linking with acid chlorides improves thermal and mechanical properties of collagen based biopolymer material. *Thermochim. Acta* **2011**, *525*, 50–55. [CrossRef]
31. Sargent, J.M. The use of the mtt assay to study drug resistance in fresh tumour samples. In *Chemosensitivity Testing in Oncology*; Springer Berlin Heidelberg: Berlin, Germany, 2003; Volume 161, pp. 13–25.
32. Silva, A.E.; Marcelino, H.R.; Gomes, M.C.S.; Oliveira, E.E.; Nagashima-Junior, T.; Egito, E.S.T. Xylan, a promising hemicellulose for pharmaceutical use. In *Products and Applications of Biopolymers*; Verbeek, C.J.R., Ed.; InTech: Rijeka, Croatia, 2012; Volume 1, p. 220.
33. Ebringerova, A.; Heinze, T. Xylan and xylan derivatives—Biopolymers with valuable properties. 1. Naturally occurring xylans structures, procedures and properties. *Macromol. Rapid Commun.* **2000**, *21*, 542–556. [CrossRef]
34. Sorg, O. Oxidative stress: A theoretical model or a biological reality? *Comptes Rendus Biol.* **2004**, *327*, 649–662. [CrossRef]
35. Williams, D.F. On the mechanisms of biocompatibility. *Biomaterials* **2008**, *29*, 2941–2953. [CrossRef] [PubMed]